# Experimental Study of Instability Modes in a Three-Dimensional Boundary Layer

H. Bippes* and P. Nitschke-Kowsky*
*Institute for Experimental Fluid Mechanics, Göttingen, Germany*

**Traveling waves in an unstable three-dimensional boundary layer are studied experimentally with the use of hot-wire anemometry. For the sake of realistic comparisons with stability theory, the tests were performed on a swept flat plate where infinite swept-wing conditions were approximated by means of contoured end plates. The required pressure gradient was imposed by a displacement body. The Reynolds number for the first appearance of traveling waves is roughly the same as that of stationary vortices. The frequencies of the most amplified waves depend on the Reynolds number. It is shown with the aid of a twin probe that in a more strongly amplified state, the traveling waves propagate in a direction different from that of the mean flow. Further upstream, where stationary waves first become visible in the oil-flow pattern, a uniform direction could not be identified. Under certain conditions, traveling waves of two frequency ranges are amplified that propagate in different directions. The present work is part of the transition experiment started at the DFVLR. It is closely connected to the theoretical work by Dallmann and Bieler.[1]**

## Nomenclature

| | |
|---|---|
| $c$ | = chord length of the flat plate |
| $c_p$ | = pressure coefficient |
| $c_r$ | = phase velocity |
| $f$ | = frequency of traveling waves |
| $\sqrt{G_{11}} = \sqrt{\overline{S_1 S_1^*}}$ | = rms spectrum |
| $G_{12} = \overline{S_1 S_2^*}$ | = average cross spectrum of $q_1(t)$ and $q_2(t)$ |
| $H_{12}$ | = shape factor |
| $Q$ | = mean velocity in the boundary layer |
| $Q_e, U_e$ | = velocity of the external flow |
| $Q_\infty$ | = freestream velocity |
| $q'$ | = root-mean-square value of $q(t)$ |
| $q(t)_{1,2}$ | = instantaneous disturbance velocity in the direction of the external flow measured on the two hot wires of the twin probe |
| $R_{12}$ | = cross-correlation function |
| $Re_\eta$ | = attachment line Reynolds number with $\eta = [\nu/(\mathrm{d}\eta_e/\mathrm{d}x)_{x=0}]^{1/2}$ |
| $Re_c$ | = freestream Reynolds number based on model chord |
| $S_i$ | = $\lvert S_i\rvert \cos(\phi_1) + j\lvert S_i\rvert \sin(\phi_1)$ complex spectrum of time history, $q_1(t)$ |
| $U,V,W$ | = components of mean boundary-layer flow in $x,y,z$ directions |
| $x,y,z$ | = Cartesian model coordinates normal and parallel to the leading edge and normal to the surface, respectively |
| $\Delta\phi$ | = average phase shift between signals $q_1(t)$ and $q_2(t)$ |
| $\delta$ | = boundary-layer thickness of the streamwise flow |
| $\lambda_S$ | = wavelength of stationary vortices |
| $\lambda_T$ | = wavelength of traveling waves |
| $\tau$ | = time lag between hot-wire signals $q_1(t)$ and $q_2(t)$ maximizing the cross-correlation function $R_{1,2}(\tau)$ |
| $\phi_0$ | = geometric sweep angle |
| $\phi(x)$ | = local sweep angle |
| $\phi_R$ | = angular position of the twin probe measured with respect to the tunnel axis |
| $\chi = V_{\max}\Delta/\nu$ | = cross-flow Reynolds number $V_{\max}$ = maximum value of cross-flow velocity; $\Delta = \int_0^\infty V/V_{\max}\,\mathrm{d}z$. (Here $V$ and $V_{\max}$ are measured normal to the external streamline and normal to the wall.) |

## I. Introduction

In previous experiments regarding the stability of three-dimensional boundary layers, the main emphasis was placed on the development of disturbance waves stationary relative to the surface and with axes laying in the streamwise direction. They are characterized as cross-flow instabilities. The work was inspired by the original observations of Gray[2] and Anscombe and Illingworth[3] on swept-wing configurations in flight tests and wind-tunnel experiments, respectively. They identified in sublimation patterns regularly spaced striations with axes lying roughly in the streamwise direction. It was suggested that the appearance of these striations is due to the existence of stationary streamwise vortex disturbances in the boundary layer, and that those may lead to transition in boundary layers with cross-flow at freestream Reynolds numbers smaller than expected. Gregory et al.[4] on a rotating disk, Poll[5] on a yawed cylinder, Arnal et al.[6] on a swept wing, Saric and Yeates[7] and Nitschke-Kowsky[8] on swept flat plates investigated this type of instability in detail.

According to stability analysis by Gregory et al.,[4] Arnal et al.,[9] Malik and Poll,[10] Dallmann and Bieler,[1] and Bieler,[11] however, traveling waves are also amplified and may play an even more important part in the transition process than the stationary vortices. Arnal et al.[6] measured in their experiments on an infinite swept wing velocity fluctuations of high intensity (15 to 20% of the external flow velocity). The observations of Poll[5] on a yawed cylinder and Nitschke-Kowsky[8] on the swept flat plate indicated that the frequencies of the traveling waves depend on the Reynolds number. Furthermore, comparison between the measurements of Nitschke-Kowsky[8] and the stability analysis of Bieler[11] ap-

Received Dec. 8, 1988; revision received Oct. 26, 1989. 

*Scientist, Deutsche Forshungs- und Versuchsanstalt für Luft- und Raumfahrt (DFVLR).

plied to the model of Nitschke-Kowsky showed that in the initial state of amplification, traveling waves develop with frequencies corresponding to those predicted by linear stability theory (see also Dallmann and Bieler[1]).

As was also revealed by Bieler's analysis, the direction of wave propagation spreads over a wide range instead of being confined to the mean flow direction, as in the initial state of amplification in unstable two-dimensional boundary-layer flows. Such a model is rather intricate, and for further understanding of the transition process, it is of special interest to provide more details concerning the occurrence and propagation of traveling waves in three-dimensional boundary layers. Thus, in the present experiment additional hot-wire measurements have been performed on the swept flat-plate model already used by Nitschke-Kowsky.[8] This configuration was chosen for being as close as possible to the simplfied mathematical model on which Bieler's stability analysis is based.

## II. Apparatus and Method

### Wind Tunnel

The present investigation was conducted in the 1-m wind tunnel at the DFVLR. It is a wind tunnel with a closed circuit and an open test section of 1 m × 0.7 m. The area reduction from the settling chamber to the test section is 4.8:1. The steadiness of the stream is improved by guide vanes and a honeycomb. Reduction of turbulence is obtained by installing three damping screens with an open area ratio of 0.65 into the settling chamber 5.1 m ahead of the nozzle exit. The turbulence level in the test section was lower than 0.15%.

### Swept Flat Plate

A swept flat plate was chosen for the tests in order to create a base for realistic comparisons with the stability calculations of Bieler[11] (Fig. 1). The cross-flow was generated by a displacement body that imposes a negative pressure gradient on the flat-plate flow. For simulating quasi-infinite-cylinder flow conditions, contoured endplates were used. For further details, see Nitschke-Kowsky.[8] For the present tests, the model was set at a sweep angle of $\phi_0 = 45$ deg.

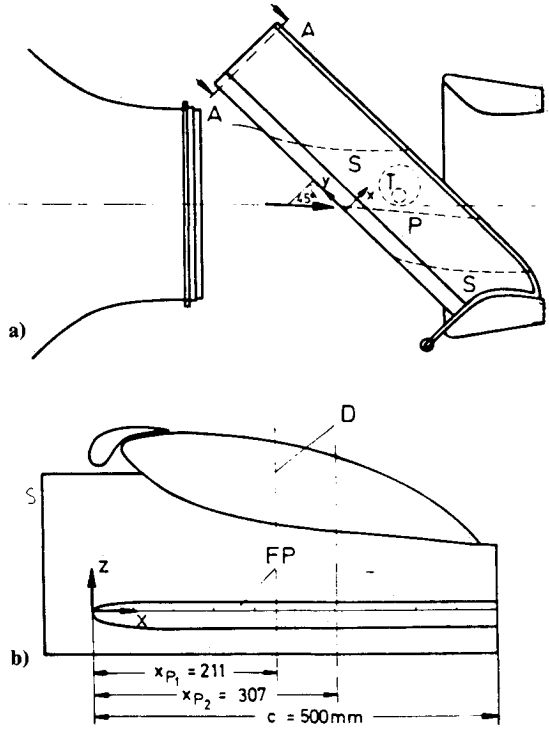


**Fig. 1 a) Swept flat-plate model in the 1-m wind tunnel. b) Model section *A-A*. *D* = displacement body, *FP* = flat plate, *P* = pressure tappings, *S* = end plate, *T* = traversing mechanism, $x_{P1}$ and $x_{P2}$ = locations of hot-wire measurements.**

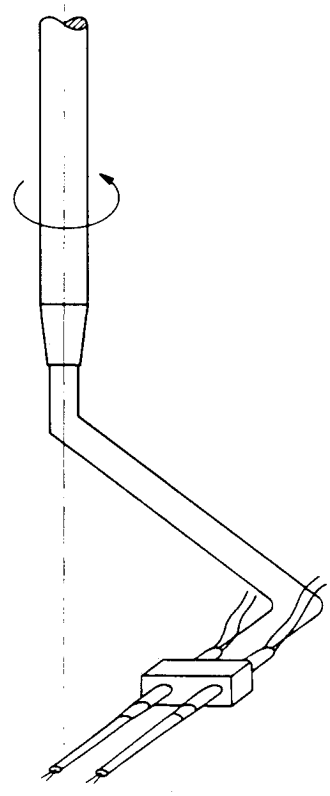

**Fig. 2 Rotatable twin probe with two hot wires 12 mm apart from one another.**

### Measurements

The measuring techniques used are described by Nitschke-Kowsky[8] in detail. Mean velocity distributions and traveling waves were traced with the aid of hot-wire anemometers. In order to detect the direction of wave propagation, two hot-wire probes were arranged on a rotatable support (Fig. 2). The distance between the two probes could be set by choice at 12 or 21 mm. With the aid of this twin probe, the direction of wave propagation was found by determining the phase shift between the instantaneous signals of the two hot wires for different angular positions of the probe support. Phase shifts were determined by means of cross-spectra and cross-correlations using a frequency analyzer. The direction of wave propagation was then identified by the position of zero phase shift between the instantaneous signals of the two hot wires. Frequency spectra were also measured. The results are presented in time-averaged values.

The rotatable twin probe was placed at two chordwise positions $x_{P1} = 211$ mm and $x_{P2} = 307$ mm from the leading edge. The angular position is varied between $\phi_R = -14$ and 108 deg. The $\phi_R$ is measured as the sweep angle, with respect to the tunnel axis. The appearance and local spanwise spacing of stationary vortices at the two measuring positions were visualized with the oil-flow technique.

## III. Results

### Mean Flow

The chordwise variation of the wall pressure on the flat plate as induced by the displacement body is shown in Fig. 3. For comparison with pressure distributions appearing on swept wings, the wall pressure measured on the lower side of a NACA 0010 airfoil is also given.

Based on the experimental pressure distribution and with infinite sweep conditions assumed, the magnitude and direction of the external flow velocity was calculated. As described by Nitschke-Kowsky,[8] close agreement between measured and calculated flow data was obtained (within 1 deg in direction and 2% in magnitude of the external flow velocity) if an effective sweep angle of 46.3 deg was assumed instead of the geometrical sweep angle of 45 deg. For chordwise positions $x/c > 0.8$ and spanwise positions close to the back-sited end plate, increasing discrepancies between calculation and measurement were observed.

In order to be able to compare the results of the stability analysis for the swept flat-plate model and the present experiment, Bieler[11] calculated the boundary-layer flow using the experimental pressure distribution. Experimental results are nondimensionalized with the calculated flow parameters in order to facilitate comparisons with theory and other experiments.

It should be further mentioned that the Reynolds number $Re_\eta$ for the attachment line flow, determined from the measured pressure distribution around the nose, was subcritical for the total range of freestream velocities adopted for the present tests (see Ref. 8).

The attachment line was located on the side of the flat plate where the measurements were performed. Therefore, no high suction peak with a subsequent strong adverse pressure gradient is generated. Thus, any small disturbances in the oncoming flow should be damped in the front part of the model.

### Stationary Waves

In order to know the ambient flowfield at the locations where the traveling waves were studied, the occurrence of stationary waves was traced with the aid of the oil-flow

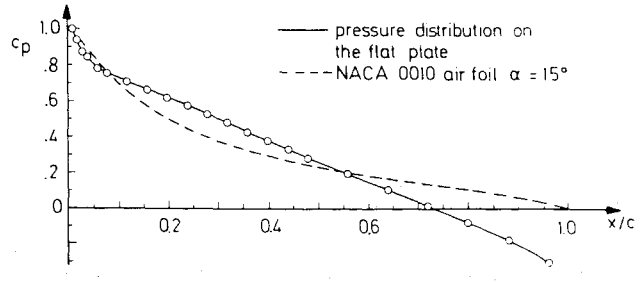


**Fig. 3 Pressure distribution measured on the swept flat plate in comparison with the pressure distribution of a NACA 0010 airfoil.**

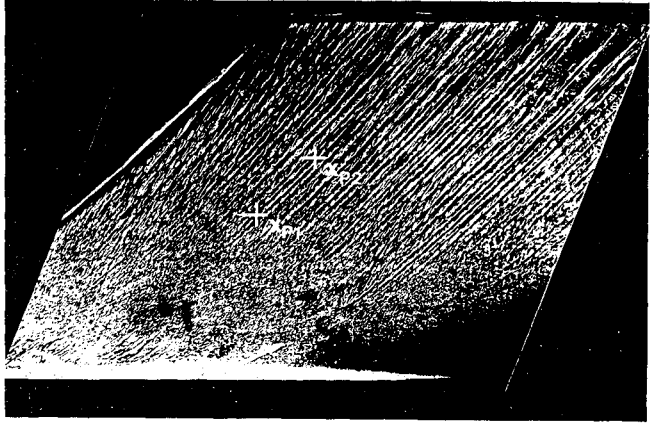

**Fig. 4 Oil-flow pattern on the swept flat-plate model; $\phi_0 = 45$ deg, $Re = 6 \times 10^5$, $x_{P1}$ and $x_{P2}$ are the measuring positions of the twin probe.**

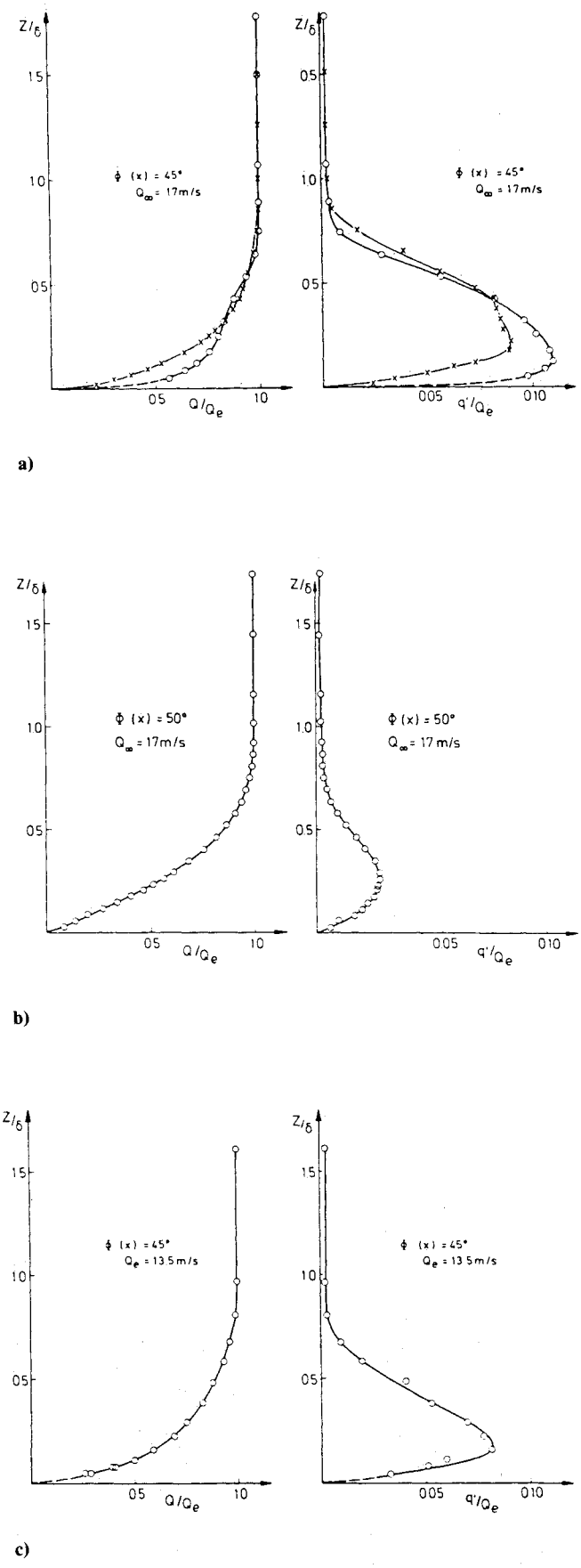


**Fig. 5 Mean velocity and disturbance profiles projected into an $x$-$z$ plane parallel to the direction of the external flow; $\phi_0 = 45$ deg. a) $Re_c = 6 \times 10^5$, $\chi = 123$, $x = x_{P2}$, $y = y_{P2}$, $y_{P2} + \lambda_S/4$. b) $Re_c = 6 \times 10^5$, $\chi = 101$, $x = x_{P1}$, $y = y_{P1}$. c) $Re_c = 4.8 \times 10^5$, $\chi = 111$, $x = x_{P2}$, $y = y_{P2}$.**

visualization technique. Figure 4 shows a result obtained for the sweep angle $\phi_0 = 45$ deg and the freestream Reynolds number $Re = 6 \times 10^5$, at which the hot-wire measurements were also performed. The stationary waves are indicated by evenly spaced streaks roughly aligned with the flow direction outside the boundary layer. At a freestream Reynolds number of $Re_c = 6 \times 10^5$, the first occurrence of the stationary waves is observed at position $x/c = 0.42$ that corresponds to a cross-flow Reynolds number $\chi = 96$. The spanwise spacing is $\lambda_S = 9$ to 10 mm or expressed in nondimensional terms $\lambda_S/\delta = 3.3$ where $\delta$ is the boundary-layer thickness. This value roughly agrees with the results of Arnal et al.,[6] as well as with the calculations of Dallmann and Bieler[1] in which $\lambda_S/\delta$ turned out to be 3.

A quantitative insight into the effect of stationary waves on the boundary-layer flow may be obtained by mean velocity profiles as given in Fig. 5a. The profiles shown have been measured at two spanwise positions about $\lambda_S/4$ apart from one another at a distance $x_{P2} = 307$ mm downstream of the leading edge. At this location, the longitudinal streaks in the oil-flow pattern of Fig. 4, where position $x_{P2}$ is also marked, are fully developed. For both the oil-flow visualization and hot-wire measurements, the same flow conditions have been chosen. The two mean velocity profiles of Fig. 5a reveal a marked difference. Whereas one of them looks like an ordinary boundary-layer profile, the other exhibits two inflection points.

It should be pointed out that at position $x_{P1}$ where the longitudinal streaks in Fig. 4 are just being formed, inflectional profiles of the boundary-layer flow in the streamwise direction are not observed while traveling waves are already amplified as shown in Fig. 5b. The same observation is made for reduced freestream velocity at position $x_{P2}$ (Fig. 5c). It is suggested, therefore, that the difference in the shape of the profiles in Fig. 5a is mainly due to the stationary waves. Thus, the stationary waves deform the boundary layer three-dimensionally by generating streamwise zones of different stability characteristics. This deformation of the profiles may give rise to secondary instabilities as tackled theoretically by Fischer and Dallmann.[12]

### Development of Traveling Disturbances

As just shown, amplified traveling disturbances are observed at positions $x_{P1}$ where in the oil-flow pattern of Fig. 4 longitudinal streaks are just being formed. Thus, for the flow conditions of the present experiment, the Reynolds numbers $\chi$ for the first appearance of both instability modes are roughly the same. Both types of instability waves may therefore be considered primary instabilities corresponding to linear stability theory (e.g., Arnal et al.[9] and Bieler[11]). It should be noted that traveling disturbances do not affect oil-flow patterns and therefore cannot be identified in Fig. 4.

Profiles of the rms values of the traveling disturbances as measured at locations $x_{P1}$ and $x_{P2}$ are shown in Fig. 5 together with the pertaining velocity profiles. The maximum in the intensity distribution expressed in terms $q'/Q_e$ is obtained at boundary-layer heights between $z/\delta = 0.15$ and 0.20. At $z/\delta \simeq 0.8$, the disturbance intensity is decreased to the disturbance level of the external flow. Maximum rms value, shown in the disturbance profiles of Fig. 5a, is $q'/Q_e \simeq 0.1$. Such fluctuation intensities are observed in unstable two-dimensional boundary layers in the case of the artificial excitation of disturbances only close to the breakdown of three-dimensional instability structures. It should be stressed, however, that the present experiments are performed under conditions of natural transition.

Between locations $x_{P1}$ and $x_{P2}$, the traveling disturbances are amplified by a factor of 3 to 4.5 depending on the spanwise position. This amplification rate slightly exceeds that of the stationary waves as a rough estimate with the aid of the velocity profiles, as given in Fig. 5, has shown.

### Features of Traveling Disturbances

Because of the conditions of natural transition, the instantaneous hot-wire signals of the traveling disturbances are not expected to reveal single harmonic waves, but a sinusoidal motion resulting from selected amplification of random disturbances in the oncoming flow. The oscillograms in Fig. 6 representing the velocity fluctuations at location $x_{P2}$ indeed look closely sinusoidal and seem to have a predominant frequency. Thus, it is suggested that the mechanism acting in unstable two-dimensional boundary layers in some way also applies to three-dimensional boundary layers. It should be noted that at larger Reynolds numbers, the occurrence of higher harmonics or "spikes" was also observed (see Nitschke-Kowsky[8]).

The frequency spectra of Fig. 7 reveal that the actual sinusoidal disturbance motions shown in Fig. 6 do not repre-

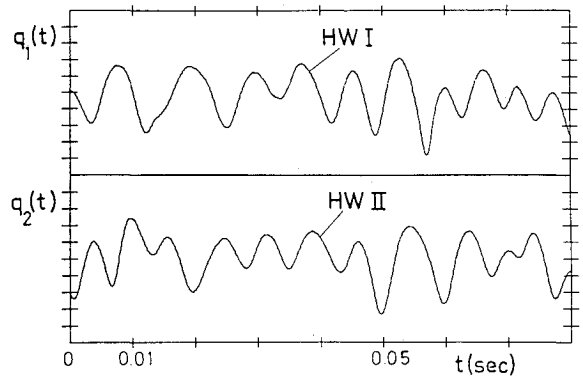


**Fig. 6 Velocity fluctuations $q(t)$ measured on the two hot wires of the twin probe; $\phi_0 = 45$ deg. $Re_c = 6 \cdot 10^5$, $\chi = 123$, $x = x_{P2}$, $z = z_{P2}$.**

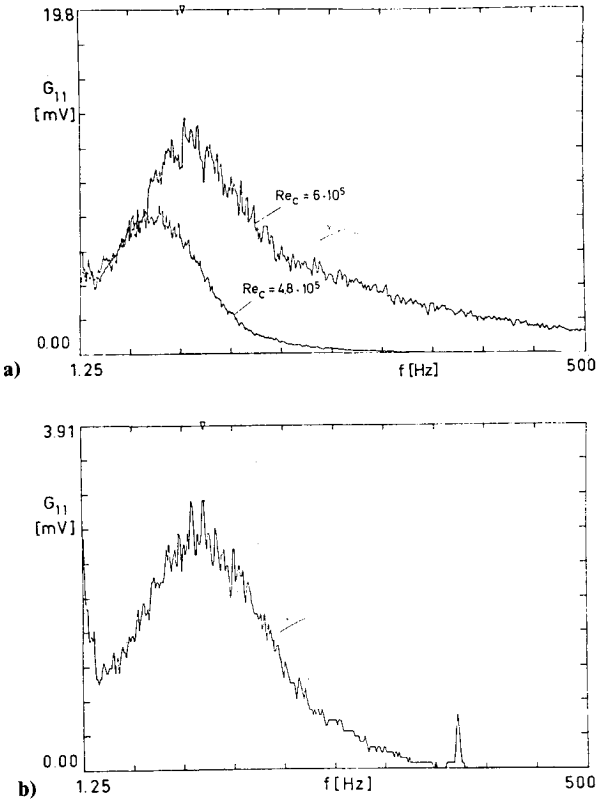


**Fig. 7 Frequency spectra of amplified traveling waves; $\phi_0 = 45$ deg. a) $Re_c = 6 \times 10^5$, $\chi = 123$, $x = x_{P2}$; $Re_c = 4.8 \times 10^5$, $\chi = 111$, $x = x_{P2}$. b) $Re_c = 6 \times 10^5$, $\chi = 101$, $x = x_{P1}$.**

sent waves of a single frequency but waves of a band of frequencies. It should be pointed out that stability calculations for our swept flat-plate model had been advanced by Dallmann and Bieler[1] to account for just such an amplification. The various spectra in Fig. 7 further indicate that the frequencies of the most amplified waves increase with the freestream velocity and slightly decrease in the downstream direction, i.e., with the growth of the boundary layer.

In order to give an idea of the effect of model vibrations on the boundary-layer flow, the appearance of model vibrations is measured with the aid of the accelerometer. Predominant peaks in the frequency spectrum (Fig. 8) occur at values $f < 35$ Hz and $f \simeq 280$ Hz. The frequencies of the most amplified disturbance waves, however, are between these limits.

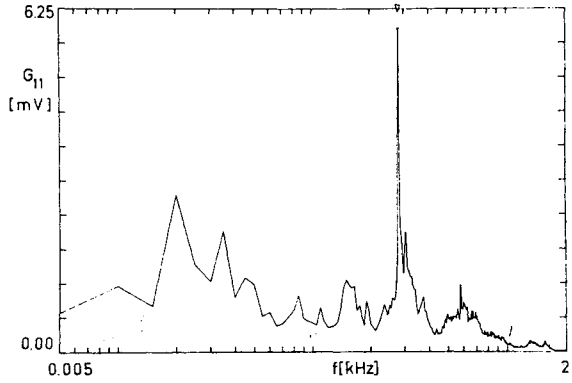


**Fig. 8 Frequency spectrum of model vibrations measured with the use of an accelerometer fixed on the flat plate.**

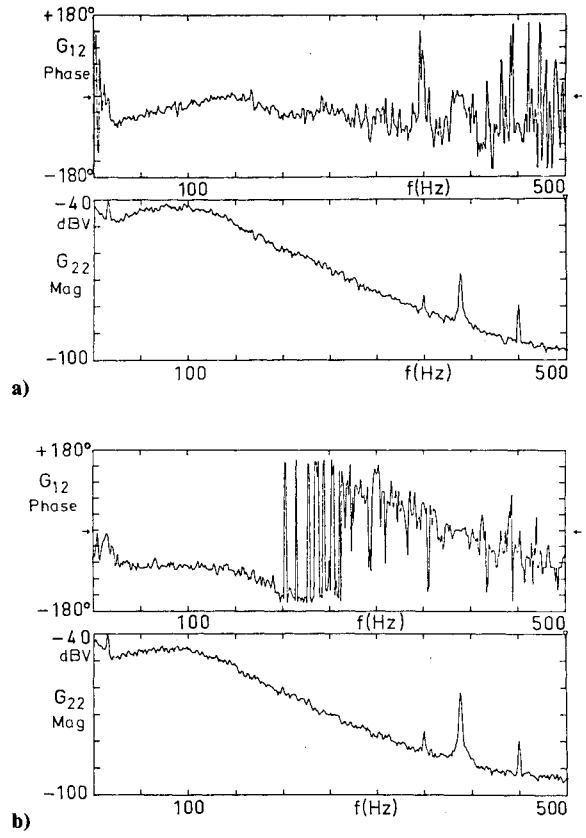


**Fig. 9 Cross spectra determined with the use of a rotatable twin probe; $\phi_0 = 45$ deg, $\phi(x) = 45$ deg, $Re = 5.3 \times 10^5$, $\chi = 117$, $x = x_{P2}$, $z/\delta = 0.05$. a) $\phi_r = 55$ deg, b) $\phi_r = 80$ deg.**

**Direction of Wave Propagation**

In order to establish whether a distinct direction of wave propagation exists, the rotatable twin probe, sketched in Fig. 2, was used as described in Sec. II. Figure 9 shows typical cross-spectra $G_{12}$ as measured at position $x_{P2}$ for two angular positions $\phi_R$ of the twin probe. The lower parts of the correlograms display the average cross-spectra of the instantaneous signals received at the locations of the two hot wires on the twin probe, and the upper parts reveal the phase shift. In the frequency range of the most amplified waves, the signals are correlated and a certain phase shift is indicated. By changing the angular position $\phi_R$ of the twin probe, the phase shift between the two hot-wire signals is also changed (compare Figs. 9a and 9b). In Fig. 10, a cross-correlation of the hot-wire signals is displayed. The appearance of a marked peak in the normalized cross-correlation function $R_{12}(\tau)$ again shows that the oscillating hot-wire signals representing the traveling waves are strongly correlated. Thus, it is suggested that the traveling waves propagate in a predominant direction.

In Fig. 10, $\tau$ indicates the time lag between the two hot-wire signals that maximizes the cross-correlation function. It is related to the phase shift displayed in Fig. 9. If $\tau$ becomes 0, the wavefronts propagate normal to the straight line connecting the two hot wires of the twin probe (Fig. 2). In order to identify this direction, cross-correlations are determined for various angular positions $\phi_R$ of the twin probe. In Fig. 11, the results are shown for three different freestream Reynolds numbers. It turns out that $\tau$ varies with $\phi_R$ and that there is a minimum value $\tau$ for each freestream Reynolds number. For the interpretation of these correlation measurements, it must be taken into account that the amplified stationary waves deform the boundary-layer flow periodically in the spanwise direction.

As a consequence, the wavefronts of the traveling waves are

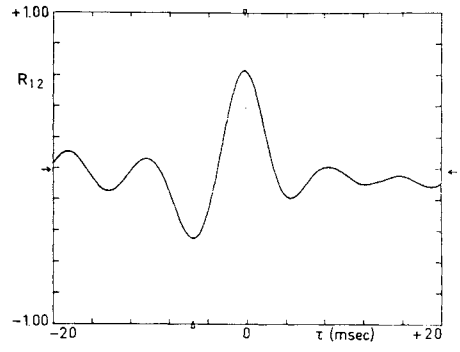


**Fig. 10 Cross-correlation function; $\phi_0 = 45$ deg, $Re_c = 5.3 \times 10^5$, $\chi = 117$, $\phi_R = 25$ deg, $x = x_{P2}$, $z/\delta = 0.15$.**

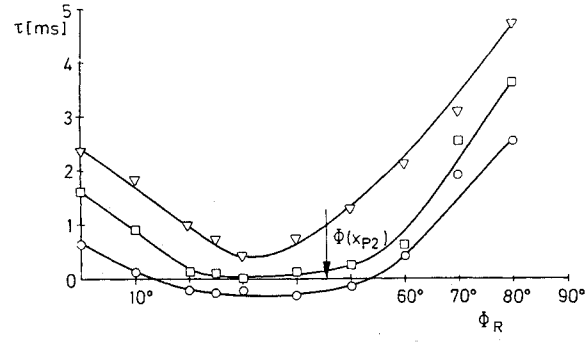


**Fig. 11 Time lags between the hot-wire signals for various rotating positions $\phi_R$ of the twin probe; $\phi(x_{P2})$ indicates the local sweep angle of the external flow; $\phi_0 = 45$ deg, $x = x_{P2}$, $z/\delta = 0.05$. ○ $Re_c = 6 \times 10^5$, $\chi = 123$; □ $Re_c = 5.3 \times 10^5$, $\chi = 117$; ▲ $Re_c = 4.8 \times 10^5$, $\chi = 111$.**

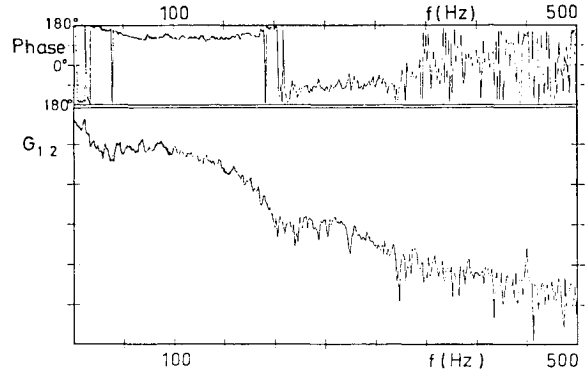


**Fig. 12 Cross spectrum with amplified traveling waves in two frequency ranges; $\phi_0 = 45$ deg, $Re_c = 8.3 \times 10^5$, $\chi = 119$, $x = x_P1$, $z/\delta = 0.05$.**

also deformed, and by rotating the twin probe the two hot wires are shifted to different positions in the deformed wavefronts. This will affect the outcome of $\tau$ shown in Fig. 11, as well as the scatter in the direction of wave propagation. Thus, it is suggested that the angle $\phi_R$ corresponding to the minimum value $\tau$ indicates the angle of wave propagation. By comparing this angle with the angle $\phi(x)$ of the local flow direction (also marked in Fig. 11), it can be seen that both angles differ from one another. This difference depends on the freestream Reynolds number. Further measurements have shown that it also depends on $z/\delta$, the measuring height within the boundary layer. It should be noted that according to linear stability theory, such a predominant direction in wave propagation does not exist (see Fig. 17 in Ref. 1).

At higher freestream Reynolds numbers, traveling waves of higher frequencies around 260 Hz are also amplified (Fig. 12). The corresponding cross-spectrum reveals that for this second band of amplified frequencies, the instantaneous signals on the two hot wires of the twin probe are also correlated. The appearance of a second bundle of amplified traveling waves may be due to the deformation of stationary waves and, therefore, may be seen as a secondary instability. Detailed measurements are necessary to explain this stage of the transition process.

## IV. Conclusions

An outstanding feature in the transition process of three-dimensional boundary layers is the appearance of traveling disturbances. Hot-wire measurements on a swept flat-plate model reveal that this instability mode originates approximately at downstream locations where stationary waves (stationary relative to the surface) first become visible in oil-flow patterns. Mean flow measurements show the spanwise periodic deformation of the boundary layer by the action of the amplified stationary waves. Therefore, streamwise zones with inflectional boundary-layer profiles develop so that the stability of the boundary layer is affected in a secondary way.

The traveling disturbances are shown to be a sinusoidal motion resulting from selected amplification of random disturbances in the oncoming flow. Frequency spectra reveal that not single waves but bands of frequencies are amplified. These frequency bands seem to be slightly broader than those found in two-dimensional boundary layers for conditions of natural transition, thus confirming the stability calculations of Dallmann and Bieler.[1] The amplified frequencies depend on the Reynolds number and on the growth of the boundary layer as it is known from two-dimensional flows.

The maximum intensity of the traveling waves is obtained at a height 15 to 20% of the boundary-layer thickness. It amounts to 11 to 12% of $Q_e$ before the "spike stage" in the transition process is reached. The amplification varies periodically in the spanwise direction, corresponding to the deformation of the boundary layer by the stationary waves.

An attempt has been made to determine the direction of wave propagation by correlation measurements using two hot wires mounted on a rotatable probe support. The result indicates that a predominant direction of wave propagation exists that differs from the mean flow direction. This statement is restricted by some uncertainties such as the three-dimensional deformation of the wavefronts and possible scatter in the propagation direction. Flow visualization and further detailed measurements are necessary in order to provide better understanding and extended quantitative results.

In a more advanced stage of the transition process, a second band of traveling waves appears in a higher frequency range. This might be due to a secondary instability.

## Acknowledgments

The authors would like to thank H. Hornung for sharing the results of his experiments. They would also like to thank B. Müller for providing additional data. The suggestions of E. Wedemeyer and G. Höhler are greatly appreciated.

## References

[1]Dallmann, U., and Bieler, H., "Analysis and Simplified Prediction of Primary Instability of Three-Dimensional Boundary Layer Flows," AIAA Paper 87-1337, June 1987.

[2]Gray, W. E., "The Effect of Wing Sweep on Laminar Flow," Royal Aircraft Establishment, TM Aero 255, Farnborough, Feb. 1952.

[3]Anscombe, A., and Illingworth, L. N., "Wind-Tunnel Observations of Boundary Layer Transition on a Wing at Various Angles of Sweep Back," Aeronautical Research Council R&M 2968, London, 1952.

[4]Gregory, N., Stuart, Y. T., and Walker, W. S., "On the Stability of Three-Dimensional Boundary Layers with the Application of the Flow Due to a Rotating Disc," *Philosophical Translations of Royal Society of London*, Vol. A248, July 1955, pp. 155–199.

[5]Poll, D. I. A., "Some Observations of the Transition Process on the Windward Face of a Long Yawed Cylinder," *Journal of Fluid Mechanics*, Vol. 150, 1985, pp. 155–199.

[6]Arnal, D., Coustols, E., and Juillen, J. C., "Etude Experimentale et Theorique de la Transition sur une Alie en Fleche Infinie," *La Recherche Aerospatiale*, July/Aug. 1984, pp. 275–290.

[7]Saric, W. S., and Yeates, L. G., "Experiments on the Stability of Cross-Flow Vortices in Swept-Wing Flows," AIAA Paper 85-0493, 1985.

[8]Nitschke-Kowsky, P., "Experimentelle Untersuchungen zu Stabilität und Umschlag dreidimensionaler Grenzschichten," DFVLR-FB 86-24, 1986.

[9]Arnal, D., Habiballah, M., and Coustols, E., "Theorie de l'Instabilite Laminaire et Criteres de Transition en Ecoulements Bi- et Tridimensionels," *La Recherche Aerospatiale*, March/April 1984, pp. 125–143.

[10]Malik, M. R., and Poll, D. I. A., "Effect of Curvature on Three-Dimensional Boundary Layer Stability," AIAA Paper 84-1672, June 1984.

[11]Bieler, H., "Theoretische Untersuchungen über primäre Instabilitäten in dreidimensionalen Grenzschichtströmungen," DFVLR-FB 84-54, 1986.

[12]Fischer, T., and Dallmann, U., "Theoretical Investigation of Secondary Instability of Three-Dimensional Boundary Layer Flows," AIAA Paper 87-1338, June 1987.